PHYSICAL REVIEW B VOLUME 12, NUMBER 4 15 AUGUST 1975

Electronic structure of S_8

W. R. Salaneck, N. O. Lipari, A. Paton, R. Zallen, and K. S. Liang
Xerox Webster Research Center, Webster, New York 14580

(Received 31 March 1975)

The electronic structure of S_8 has been studied using a complete-neglect-of-differential-overlap self-consistent-field molecular-orbital formalism. The results of the calculation are compared with our own x-ray photoemission spectra of the valence band of amorphous and polycrystalline samples consisting of thin films formed by the *in situ* vapor deposition of S_8 molecules. In addition, the calculated results adequately account for the high-resolution ultraviolet photoemission and absorption of S_8 molecules in orthorhombic sulfur as well as in the gas phase.

I. INTRODUCTION

Although cyclo-octasulfur S_8 is one of the simplest of the molecular chalcogenides, its electronic structure has received relatively little attention in the literature. Extensive studies of the transport and photoconductive properties of orthorhombic sulfur,[1] the crystal composed on only S_8 rings, have been carried out. The optical spectrum of orthorhombic sulfur has been studied by Cook and Spear,[2] and Emerald, Drews, and Zallen.[3] While the electronic structure was investigated by Nielsen[4(a)] utilizing ultraviolet photoemission spectroscopy (UPS) of solid samples made up of S_8 rings, photon energies of 21.2 eV (He I) and lower were used in the UPS study. With 21-eV photons, only the upper (lowest-binding energy) portion of the valence band can be investigated.[4(b)] The results of an extended Hückel (EH) molecular-orbital (MO) calculation by Chen[5] were employed in the analysis of the UPS spectra. Unfortunately, the results of the Hückel calculation predict a narrow valence band and an increase in electronic energy upon formation of the molecule. Earlier calculations of some of the features of the electronic structure of S_8 by Gibbons[6] involved the assumption of a π-electron system for the uppermost MO's. The results of our study and those of a gas phase UPS study by Boschi and Schmidt[7] reveal that there are no π-electron bonding MO's in S_8. Finally, since our study was completed, Richardson and Weinberger[8] have reported studies on S_8 using both x-ray photoemission spectroscopy (XPS) and UPS. Their UPS data are of lower resolution than those of Boschi and Schmidt, and their XPS data are of lower resolution than ours. Richardson and Weinberger used a self-consistent-field $X\alpha$ scattered wave calculation to interpret their data. They have not discussed the bonding character of their MO's and their energy-eigenvalue spectrum does not agree completely with the uppermost ionization potentials as seen in the high-resolution UPS data of Boschi and Schmidt.

We have carried out a semiempirical self-consistent-field (SCF) calculation of the MO spectrum of the S_8 molecule.[9] We have used the zero-differential-overlap (ZDO) method of Pople, Santry, and Segal[10] in the complete-neglect-of-differential-overlap (CNDO) approximation. The results of the computation, which will be outlined in Sec. II, are then compared with our own x-ray-photoemission-spectroscopy (XPS) data on the valence band of amorphous and polycrystalline films composed of S_8 puckered ring molecules. These samples were prepared *in situ* in the XPS spectrometer, which will be described in Sec. III. In Sec. IV, the results of the MO calculation are compared with those of the $X\alpha$ calculation and with the various XPS and UPS data on solid S_8, as well as the data on S_8 vapor. The optical spectrum of S_8 molecules is also predicted, based upon a configuration-interaction treatment of SCF MO's. The results are summarized in Sec. V.

II. THEORY

The earliest published MO calculation of S_8 is based upon extended Hückel (EH) theory.[5] Hückel theory does not include electron repulsion, the wave functions are not properly antisymmetrized,[10] and an explicit Hamiltonian is not used. Matrix elements of the Hamiltonian are written down empirically in a basis of localized bond orbitals in which the Hamiltonian is nondiagonal. The matrix is then diagonalized to obtain its eigenfunctions and eigenvalues. This renders calculated quantities, in general, basis-set dependent. Self-consistent-field (SCF) molecular-orbital (MO) theories such as CNDO and $X\alpha$, on the other hand, allow for the correct antisymmetrization of the MO wavefunction and also incorporate electron repulsion explicitly (if not exactly, in some average fashion).[11] The $X\alpha$ method was developed[12,13] to give an *ab initio* method which accurately approximates full Hartree-Fock results while requiring much less computing time. We show in this paper that CNDO-SCF not only can give somewhat more accurate results on S_8 molecules, but that the computation time is very small as compared with $X\alpha$. The CNDO and $X\alpha$ results are compared in Sec. IV.

In this paper, we present a discussion of the application of the simplest of the semiempirical SCF MO methods, the zero-differential-overlap (ZDO) method of Pople, Santry, and Segal[10] in the complete neglect of differential overlap (CNDO) as applied to S_8 molecules. The reader is referred to the extensive standard quantum literature for detailed discussions of CNDO-SCF MO theory[11,14–17] An outline of the logic and the choice of the input parameters are presented below. We follow the outline of the method as presented by Friedman.[18]

The foundation for the model most often utilized in the interpretation of photoelectron spectroscopy is based on the Hartree-Fock approximation, with molecular orbitals expressed as a linear combination of atomic orbitals (LCAO), $\psi_i = \sum_j c_{ij}\phi_j$. The c_{ij} are determined by solving the Hartree-Fock-Roothan equations[19] self-consistently. The difficulties lie in evaluation of the Fock energy matrix, the elements of which may be written

$$F_{jk} = H_{jk} + G_{jk} . \tag{1}$$

H_{jk} is the nuclear-field–one-electron interaction term, and G_{jk} represents the electron-electron interaction,

$$G_{jk} = \sum_m \sum_n P_{mn}(\langle jk\,|\,mn\rangle - \tfrac{1}{2}\langle jm\,|\,kn\rangle), \tag{2}$$

where, in Mulliken notation,

$$\langle jk\,|\,mn\rangle = \int \phi_j^*(1)\,\phi_k(1)\,(r_{12}^{-1})\,\phi_m^*(2)\,\phi_n(2)\,d\tau_1 d\tau_2 \tag{3}$$

and

$$P_{mn} = 2\sum_j{}' c_{jm}^* c_{jn} . \tag{4}$$

The sum in (4) extends only over occupied orbitals. Neglecting additive constants such as the nuclear repulsion energy, the energy eigenvalues of the system are given by

$$E_i = \sum_j \sum_k c_{ij}^* c_{ik}(H_{jk} + G_{jk}), \tag{5}$$

and the total electronic energy is given by

$$E_T = \frac{1}{2}\sum_j \sum_k P_{jk}(H_{jk} + G_{jk}). \tag{6}$$

ZDO formalisms involve the neglect of all three- and four-center electron integrals, resulting in $j = k$ and $m = n$ in (3). The CNDO approximation neglects differential overlap of atomic orbitals,[16,17] $\phi_j\phi_k = \delta_{jk}\phi_j\phi_k$. The remaining integrals are "parameterized" by utilizing analytical expressions in order to compensate in some way for the approximations outlined above. The use of empirical expressions for the electron integrals renders their values independent of the choice of atomic-orbital basis states.[20]

The parameterization used here, that due to Clark,[21] is essentially the same that we have used previously in studies of x-ray emission in As, S glasses[22,23] and of the electronic structure of the molecular arsenic chalcogenides As_4S_4 and As_4Se_4.[24,25]

The wave functions are expressed as linear combinations of s, p, and d atomic Slater-type orbitals (STO's). The one-electron contributions to the diagonal elements of $\underline{H}$ are derived from ionization potentials of atomic-energy levels[26] I_j. Because of the d orbitals,[21,27] the off-diagonal elements of $\underline{H}$ are constructed from a Wolfsberg-Helmholz relationship,[28] $H_{jk} = (I_j + I_k)KS_{jk}$, where K is an adjustable parameter whose effect will be discussed in Sec. IV. The off-diagonal elements of the two-center electron matrix $\gamma_{jk} = (jj\,|\,kk)$ are obtained from a scheme for S atoms due to Clark,[21] while the diagonal elements are constructed from the Pariser formula.[29] The molecular geometry of S_8 was taken from standard literature.[30] A diagram of the S_8 geometry is shown in Fig. 1, and the

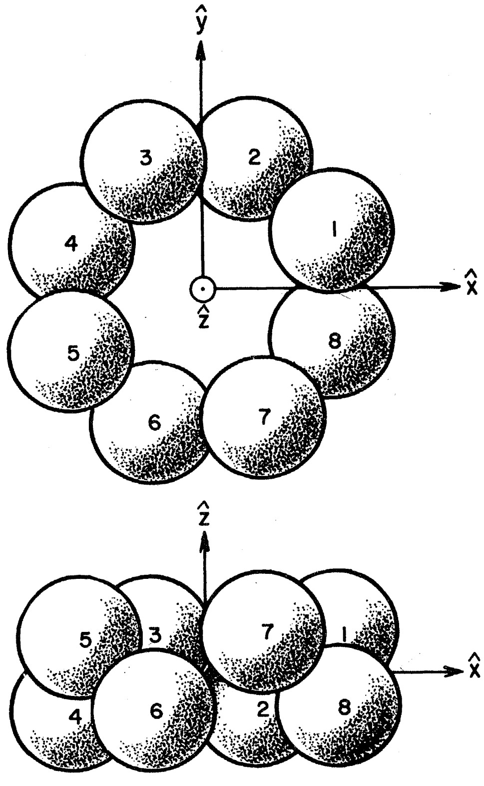

FIG. 1. Eight-membered puckered-ring structure of the S_8 molecule (Ref. 46) is shown. The molecular z axis is perpendicular to the plane of the ring, while the x and y axes lie within the plane. The point-group symmetry of the isolated molecule corresponds to D_{4d}.

TABLE I. Atomic coordinates of S_8.[a]

Atom No.	X	Y	Z
1	a	b	c
2	b	a	$-c$
3	$-b$	a	c
4	$-a$	b	$-c$
5	$-a$	$-b$	c
6	$-b$	$-a$	$-c$
7	b	$-a$	c
8	a	$-b$	$-c$

[a] The atomic coordinates of S_8 correspond to the corners of two squares 3.312 Å on a side, separated by $2c = 0.992$ Å, and rotated 90° from one another (Ref. 39). Thus, $a = 2.163\,6683$ Å, $b = 0.896\,2208$ Å, and $c = 0.496\,00$ Å. The indicated accuracy is convenient for the exact canceling of terms in determining the symmetry of the wave functions.

atomic coordinates are given in Table I.

The MO's obtained in a SCF-type calculation (the *de*localized orbitals) are eigenfunctions of the total Hamiltonian. In this basis, the total Fock energy operator is diagonal, and the eigenvalues (the energies of the individual MO's) correspond to ionization potentials.[19,31] Since relaxation effects are typically small across the valence electrons, the one-electron energies are expected to be good approximations to the valence-band photoemission energies (Koopman's theorem). On the other hand, the localized bond orbitals (hybridized orbitals), such as sp^3, etc., are related to the delocalized orbitals through a unitary transformation which leaves observables such as the total energy and the total charge distribution unchanged. In the basis of the localized bond orbitals, however, the energy operator is *not* diagonal, and thus energies associated with localized orbitals are not observables in a photoemission experiment. Optical transitions must also be calculated from the eigenstates (*de*localized orbitals) for the same reason.[16,31]

The bonding, nonbonding, or antibonding nature of the individual MO's can be determined by calculating the degree of continuity of a given MO between pairs of atoms α and β, using the overlap integral as defined by

$$s_i(\alpha, \beta) = \sum_{k} \sum_{k'} c_{ik}(\alpha) c_{ik'}(\beta) \int \phi_k(\alpha) \phi_{k'}(\beta) d\tau \ . \qquad (7)$$

The c_{ik} are the k coefficients of the atomic orbitals $\phi_k(\alpha)$ centered on atom α for a given MO Ψ_i. The sums are over the atomic orbitals of each of the neighboring atoms α and β. Since any given MO may have a node between atoms α and β, one can sum $s_i(\alpha, \beta)$ over all atom pairs for a given Ψ_i,

$$S_i = \sum{}' s_i(\alpha, \beta). \qquad (8)$$

The first few optical transitions of the S_8 molecule can be obtained from the eigenvalue spectrum. The symmetries of the occupied and the unoccupied orbitals determine the polarization dependence of the dipole-allowed transitions. A simple difference in the corresponding orbital energies is *not* sufficient to determine the transition energies, however, since electron-hole correlation effects must be included. We handle the correlation problem by employing a configuration-interaction (CI) program[15] based upon an analysis like that given by Lowitz.[32]

III. EXPERIMENT

Prior to 1975, the experimental studies of the electronic structure of S_8 involved mainly optical spectroscopy of orthorhombic sulfur[2,3] and ultraviolet photoemission of S_8 molecules.[4(a),7] The photoemission experiment measures orbital energies directly. Optical spectroscopy measures, essentially, differences in orbital energies. We have utilized x-ray-photoemission spectroscopy (XPS or ESCA) to investigate the valence-band density-of states in thin-film samples consisting of S_8 molecules. Because of the high photon energy (1253.7 eV), the XPS data extend Nielsen's UPS measurement[4(a)] to deep enough binding energy to observe the entire valence band. We also make use of the He I UPS data on S_8 molecules in the vapor phase obtained by Boschi and Schmidt.[7]

Our valence-band and core-level XPS spectra were recorded on an AEI ES 200B photoelectron spectrometer utilizing Mg (K_α) radiation, for which $h\nu = 1253.7$ eV and $\Delta(h\nu) = 0.7$ eV. Facilities for simultaneous vapor deposition and data acquisition are incorporated into the spectrometer. The conditions for vapor depositing thin films composed of S_8 molecules in either the polycrystalline or amorphous phase have been worked out by Nielsen.[4(a)] The vapor pressure of orthorhombic sulfur is about 10^{-5} Torr at room temperature[33] and consists almost entirely of S_8 puckered rings.[34] Boschi and Schmidt reported that no significant population of molecular species other than S_8 molecules exist in the vapor or orthorhombic sulfur up to 140 °C. We have prepared thin-film samples of S_8 molecules by heating a capillary tube containing powdered orthorhombic sulfur[35] to 75 °C in a vacuum with a base pressure of $< 1 \times 10^{-9}$ Torr. The rise in pressure during vapor deposition was about 3×10^{-9} Torr. Sputter cleaned gold was used as the substrate. Films formed at ~ −20 °C appeared polycrystalline, while those formed at −100 °C appeared glassy. The data are identical, however. A S($2p$) core-level spectrum is shown in Fig. 2 and a valence-band spectrum in Fig. 3. Note that the $2p_{1/2}$ and $2p_{3/2}$ lines are nearly resolved. The XPS data obtained with Al(K_α)

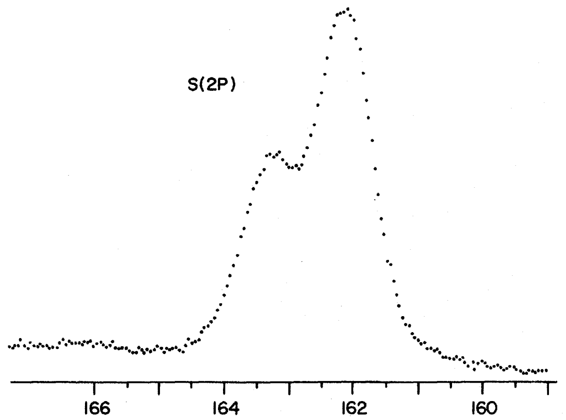

FIG. 2. The XPS spectrum of the S(2*p*) core level is shown. The binding energy of the $S(2p_{3/2})$ line, 162.25 ± 0.15 eV, is an average value for five separate samples. The sample-to-sample variation is within the ± 0.15 eV limits. The $S(2p_{1/2}) - S(2p_{3/2})$ splitting is 1.15 ± 0.05 eV. The energy is referenced to the $Au(4f_{7/2})$ line at 83.8 eV (Ref. 35), as described in the text.

radiation[8] do not resolve the spin splitting of the S(2*p*) level. The same energy resolution difference applies to the XPS valence-band data.

Energy calibration and film-thickness control was achieved by observing, for example, the S(2*p*) core-level spectrum during vapor deposition, e.g., ~1 Å/min. For sample thickness such that the Au(4*f*) levels could still be observed, the S(2*p*) energies were referenced to the $Au(4f_{7/2})$ line at 83.8 eV.[36] Vapor deposition was then continued until the Au(4*f*) lines could no longer be observed and then either terminated or continued at ~0.1 Å/min to maintain a fresh surface. Subsequent observation of the reference core levels indicated that no sample charging occurred in these thin films. The S(2*p*) data are shown in Fig. 2. Final thicknesses were estimated to be < 100 Å. At the end of an all-day run, the C(1*s*) signal was negligible and O(1*s*) was not detectable.

IV. RESULTS

The CNDO-SCF MO's of the S_8 molecule, as labeled by the irreducible representations of D_{4d}, the molecular point-group symmetry, and the corresponding energy eigenvalues, are displayed in Table II. The XPS valence-band density of states of S_8 is calculated by plotting the energy-eigenvalue spectrum broadened by 1 eV Gaussian function. This CNDO-SCF theoretical density of states is also shown in Fig. 3. Since neither the XPS nor the UPS data on solid films of S_8 molecules can resolve the individual MO energy levels, one must turn to the high-resolution UPS studies of S_8 molecules in the vapor phase. The upper portion of our MO energy spectrum is shown in detail in Fig. 4, along with the high-resolution vapor-phase data of Boschi and Schmidt[7] and Nielsen's UPS data[4] on solid films of S_8. We first illustrate the agreement between the CNDO-SCF results and photoemission experiments and then discuss the variation of parameters to achieve this agreement. Finally, we present the corresponding optical spectrum without further parameter readjustment.

As can be seen in Fig. 3, the calculated density of states agrees well with the features of the XPS valence-band data. The relative magnitudes of the XPS peaks can be used to determine the relative cross sections for photoemission for 1253.7-eV photons by considering the relative contribution of the 3*s* and 3*p* electrons to the individual photoemission peaks. Table III shows the relative 3*s* and 3*p* origin of each peak, as labeled in Fig. 3. The data of Table III were determined by summing the

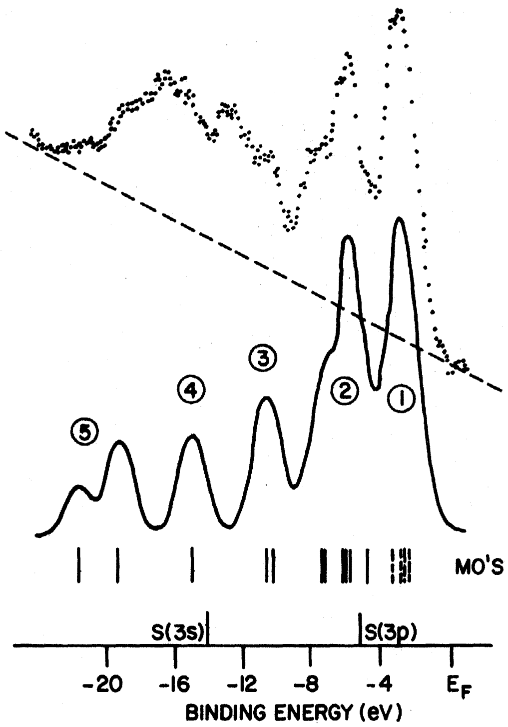

FIG. 3. The XPS data on the valence band of films of S_8 molecules are shown as data points. A plausible straight-line approximation to the inelastic background is shown as a dashed line. The density of states, as derived by broadening the CNDO-SCF eigenvalue spectrum with 1-eV Gaussians, is shown as the solid curve. Note the positions of the valence-state ionization potentials (Ref. 26) used as inputs into the program. Peak No. 1 corresponds entirely to nonbonding orbitals, while Peak No. 2 corresponds to bonding orbitals, both of mostly 3*p*-electron origin.

TABLE II. Eigenvalue spectrum of S_8 molecules.

MO[a]	Symmetry[b]	E	Bonding[c]
31, 32	e_1	+0.82	a
30	b_2	+0.78	a
28, 29	e_2	+0.50	a
27	b_2	−0.17	a
25, 26	e_2	−0.19	a
23, 24	e_3	−9.11	n
22	a_1	−9.38	n (π)
20, 21	e_2	−9.63	n
18, 19	e_1	−10.13	n
17	b_2	−11.65	b
15, 16	e_2	−12.35	b
14	a_1	−12.46	b
12, 13	e_1	−12.58	b
10, 11	e_3	−14.16	b
9	a_1	−14.34	b
8	b_2	−16.73	b
6, 7	e_2	−17.52	b
4, 5	e_2	−21.53	b
2, 3	e_2	−25.85	b
1	a_1	−28.27	b

[a] The one-electron orbitals are numbered from 1-24 for the occupied orbitals and higher for the unoccupied orbitals. Only a few of the 48 unoccupied are included.

[b] The symmetries are labeled by the irreducible representations of D_{4d}.

[c] The antibonding (a), bonding (b), or nonbonding (n) character of the orbitals is indicated. The (π) designation indicates the only orbital which is pseudo-π-like, but which is nonbonding because of the shift of neighboring S atoms according to the puckered-ring geometry.

squares of the coefficients of the atomic orbitals for each of the MO's whose energy falls under a given photoemission peak. The resultant cross-section ratio is $\sigma(3s)/\sigma(3p) = 0.8$. With 21.1-eV photons, peak No. 3 should have appeared in Nielsen's UPS data if the cross-section ratio is the same at 21.2 eV as at 1253.7 eV. Since this peak does not appear and is ~67% of 3s origin, Nielsen has concluded that the cross-section ratio is significantly different at 21.2 eV, with $\sigma(3s) \ll \sigma(3p)$.

Table III also illustrates the separation in energy of bonds that arise from initial 3s and 3p electrons in S_8. The 3s-derived levels are not, however, corelike. A computation of the molecular-overlap functions, using Eq. (8), indicates that the orbitals labeled "b" in Table II are bonding MO's by virtue of a large overlap ($S_i = 0.3$ to 0.4), while those labeled "n" are nonbonding MO's by virtue of a small overlap ($S_i \leq 0.01$). The lowest in energy (largest binding energy) MO's are mostly of 3s origin and correspond to bonding ring-quantized-type orbitals similar to those used by Platt[37] in modeling the π electrons in benzene. The bonding orbitals in S_8, however, all correspond to σ-type bonds. No π-like bonding orbitals are found. One orbital, No. 22, is pseudo-π-like to the extent that the wave function is p_z-like on each atom. Because of the pucker in the S_8 ring, however, the

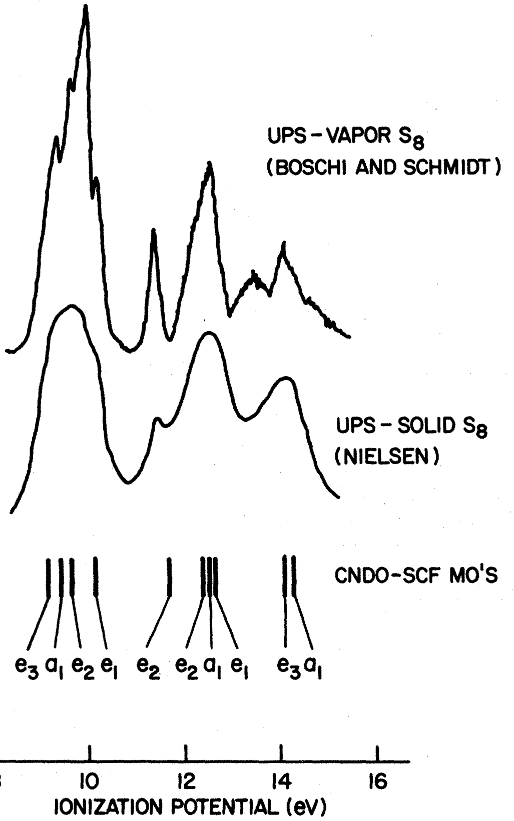

FIG. 4. UPS data on a vapor of S_8 molecules by Boschi and Schmidt (Ref. 7) are shown at the top. The data were acquired on a Perkin-Elmer Model PS-18 instrument. The center curve represents the UPS on solid films of S_8 molecules by Nielsen (Ref. 4). The vertical lines indicate the positions in energy of the uppermost MO energies, as obtained from the CNDO-SCF calculation, and are labeled by the irreducible representations of D_{4d}.

TABLE III. Atomic 3s and 3p origin of the valence-band peaks of S_8.[a]

Peak No.[b]	Percent 3s	Percent 3p
1	3	97
2	8	92
3	67	33
4	70	30
5	86	15

[a] Since the 3d orbitals contribute no more than 1% to any XPS peak, they have not been included above. The entries in the table have been rounded off to the nearest whole percent.

[b] See Fig. 3

overlap is very small, and this orbital corresponds to a nonbonding eigenstate. Additionally, the *p*-derived orbitals can be divided into two groups: nonbonding MO's ($S_i \approx 0.01$) that account for the first x-ray photoemission peak, and bonding MO's ($S_i \approx 0.2$) that produce the second x-ray photoemission peak, as labeled in Fig. 3. The energy separation of the *p*-derived bonding and nonbonding orbitals in S_8 is the same as that which occurs in the twofold coordinated chainlike chalcogens, tellurium and trigonal Se[58] and is consistent with the current picture of lone-pair semiconductors.[39,40] The states originating from the 3*s* electrons are, however, *bonding*. This differs from the results of pseudopotential calculations on Te and Se (chains)[38] and from Kastner's viewpoint.[40] The 3*s* states experimentally appear to contribute to bonding by virtue of the broadness of the XPS spectrum in the region of the 3*s* ionization potential. Additionally, through the *n*-effective sum-rule analysis of optical data[3] on orthorhombic sulfur, the 3*s* electrons are found to participate in the bonding.

The need for the inclusion of the unoccupied 3*d* orbitals in MO calculations on sulfur-containing molecules has been discussed by several authors.[21,27,41] The role of the 3*d* states in S_8 was determined in the following manner: Since Clark[21] found that the 3*d* states could be parameterized in the same fashion as the 3*p* states, our initial parameterization consisted of the Slater exponents according to the calculated values of Burns.[42] The ionization potentials for the atomic 3*s* and 3*p* states, −20.77 V and −11.88 eV, respectively, were taken from the standard literature[26] and not adjusted. The ionization potential for the 3*d* states was the value used by Clark in modeling the ground-state properties of thiophene,[21] −2.0 eV. The Slater exponents (ζ) and the Wolfsberg-Helmholz parameter (K) were then varied over small ranges in order to bring the upper MO's into the best possible agreement with the data of Boschi and Schmidt. The optimized parameters are $\zeta_{3s}=1.70$, $\zeta_{3p}=1.70$, $\zeta_{3d}=1.52$, with $K_{3s}=0.5$ and $K_{3p}=K_{3d}=0.7$. The use of the optimized parameters does not increase the (previously minimized) total ground-state energy. The main effect of varying these parameters is to change the energy spacing of the eigenvalue spectrum in a nonlinear fashion. The symmetries and bonding properties are not affected. On the other hand, a slightly better fit to the gas phase UPS data can be obtained by either not using the *d* orbitals ($\zeta_{3d} \to \infty$) or by letting $K=0.7$ for 3*s*, 3*p*, *and* 3*d*, while simultaneously readjusting ζ_{3s} and ζ_{3p}. In either case, the parameterization for a slightly better fit also results in an increase in the total ground-state energy of the molecule, and an increase in the width of the valence band to a degree greater than that observed. The 3*d* orbitals, however, make no more than a 1% contribution to any of the XPS peaks of Fig. 3.

TABLE IV. Optical transitions in S_8 molecules.

E (eV)	Symmetry[a]	Oscillator strength[b]
3.6	B_2	0.08
4.1	E_1	0.45
5.6	E_1	0.08
6.3	E_1	0.01

[a] The symmetries are labeled by the irreducible representations of D_{4d}. B_2 corresponds to photon polarization along the z axis of the *molecule*, while E_1 corresponds to polarizations within the x-y plane.

[b] The oscillator strengths are computed using Slater-type orbitals and thus are only zeroth-order approximations.

The first few optical transitions associated with the S_8 molecule were obtained from the orbital eigenvalue spectrum using the configuration-interaction (CI) program, where seven occupied and three unoccupied wave functions were utilized in the initial manifold. The allowed singlet transition energies, along with their oscillator strengths, symmetries, and corresponding polarizations, are given in Table IV. The calculated oscillator strengths are useful only to zeroth order, however, due to the use of Slater-type orbitals in the computation. Note that the polarizations refer to the coordinate axes of the *molecule*. Our predictions for optical transitions in S_8 molecules can be compared to experimental data, but we do not expect exact agreement since the optical-absorption data available[2,3] were obtained from single crystals of orthorhombic sulfur. In the crystal, there are four S_8 molecules per unit cell with translationally-inequivalent orientations.[43] The *crystal* symmetry of rhombic sulfur is D_{2h} (*Fddd*), and each molecule occupies a site of C_2 symmetry so that its environment is of much lower symmetry than the D_{4d} symmetry of an isolated S_8 ring. In this complex situation, in which there are several molecules per unit cell *and* a lowered-symmetry environment of each molecule, we have to contend with a combination of Davydov[44] and crystal-field splittings.[45]

A high degree of correspondence does exist, however. The optical data of Emerald, Drews, and Zallen[3] are shown in Fig. 5. We find that the lowest energy peak in the imaginary part of the dielectric constant (ϵ_2) for orthorhombic sulfur occurs at about 4.2 eV, independent of the photon polarization relative to the *crystallographic* axes. This energy coincides with the first (strong) tran-

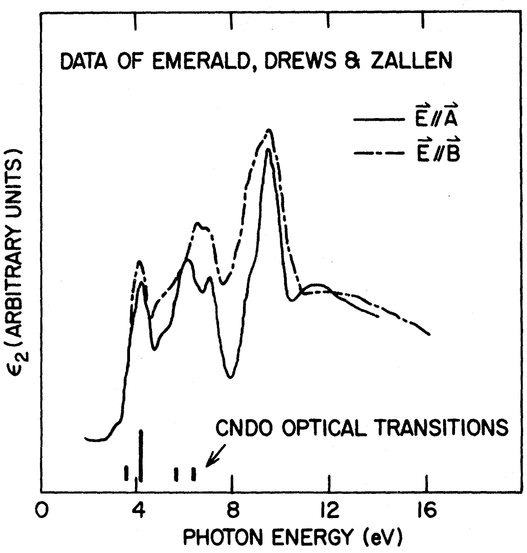

FIG. 5. Imaginary part of the dielectric constant for α-orthorhombic sulfur is shown. The data were obtained by Emerald, Drews, and Zallen (Ref. 3) using polarized light in reflectivity measurements on natural faces of orthorhombic sulfur. ϵ_2 was determined from the usual Kramers-Kronig analysis. The vertical bars indicate the energies of the first few singlet optical transitions for S_8 molecules, as taken from Table IV.

sition of E_1 symmetry as computed for the S_8 molecule. Considering the packing arrangement of the S_8 molecules in the unit cell of orthorhombic sulfur,[46] photons should couple to this mode in the molecule for all possible photon polarizations relative to the crystallographic axes. This point is consistent with the optical data of Fig. 5. At higher photon energies, structure in ϵ_2 is polarization dependent even for the photon $\vec{E}$ vector within the a-b plane. Since the unit-cell packing of the molecules would indicate a photon coupling to both the E_1 and B_2 modes for polarization either parallel to the a axis *or* the b axis and thus identical spectra for the two polarizations, the slight difference in higher-energy (>4.2 eV) structure in ϵ_2 must be a result of a solid-state-induced splitting. Our computation also predicts a weak B_2 transition around 3.6 eV. If this transition is not affected by the incorporation of S_8 molecules into the orthorhombic unit cell, it should appear in optical data for the photons polarized in the a-b plane but *not* for photons polarized parallel to the c axis. Unfortunately, the optical data for $\vec{E} \parallel \vec{c}$ are still incomplete. The data of Baer and Carmack[47] acquired on S_8 molecules in hexane are of too low resolution to be of use for this purpose.

It is obviously important to compare the results of our study on S_8 with those of Richardson and Weinberger.[8] Both the CNDO-SCF and the $X\alpha$ methods are self-consistent-field methods. The CNDO is semiempirical, while the $X\alpha$ is more *ab initio*.[12,13] The $X\alpha$ method was originally designed to be an accurate approximation to, and computationally efficient, as compared to the Hartree-Fock results on a given system.[12] It is not always obvious, however, how to parameterize the "muffin-tin" approximation or the local- (statistical) exchange approximation, especially for covalent materials. In addition, only 6 min of central-processing-unit time is required to run the CNDO calculation once on a modest Xerox Σ-7 computer, and less than one minute on an IBM/360—times which are very short compared to an $X\alpha$ computation. Finally, the two most important aspects of all are (i) the upper four ionization potentials that form the first UPS band are quite accurately accounted for with the CNDO-SCF calculation, while the $X\alpha$ computation only yields three ionization potentials in the first UPS band, and (ii) the calculated optical spectrum of Richardson and Weinberger predicts 16 transitions within approximately the same energy range as our four. Since no estimate of oscillator strengths was given, the significance of so many transitions is not obvious, and they do not compare particularly favorably with the optical data shown in Fig. 5.

V. SUMMARY

We have carried out the most computationally accurate study of the electronic structure of S_8 molecules to date. The use of 1253.7-eV x-ray photons for the photoemission spectroscopic study of films composed of S_8 molecules enabled the observation of the entire valence band, albeit with low resolution. The data have been interpreted utilizing a semiempirical self-consistent-field molecular-orbital calculation, within the complete-neglect-of-differential-overlap approximation, of the single-electron eigenfunctions and corresponding energies of the S_8 molecule. The parameterization was adjusted so that the uppermost molecular-orbital energies are in good agreement with the published high-resolution ultraviolet-photoemission data on S_8 molecules in the vapor phase. A configuration-interaction treatment of the resultant orbital eigenvalue spectrum has been used to estimate the first few singlet transitions in the optical spectrum of S_8 molecules.

The features of the electronic structure of S_8 molecules that have been revealed by this study include: the absence of any π-type bonding orbitals; the existence of only one pseudo-π nonbonding orbital; the fact that the 3s orbitals are a part of the valence band and contribute to the ring-quantized-type bonding states of the lower valence band; and the upper valence band is derived almost entirely from the S(3*p*) orbitals, the top portion corresponding to nonbonding orbitals that are responsible for the lowest-binding-energy XPS valence-band peak, and the next (higher-binding-energy) portion resulting from bonding orbitals.

VI. ACKNOWLEDGMENTS

The authors are grateful to Professor D. Clark of the University of Durham, U. K. for supplying the initial version of the CNDO-SCF computer program and to C. B. Duke, P. Nielsen, I. Chen, and Professor Clark for many helpful discussions.

---

[1] See for example, W. E. Spear and A. R. Adams, in *Elemental Sulfur*, edited by B. Meyer (Interscience, New York, 1965), Chap. 10.

[2] B. E. Cook and W. E. Spear, J. Chem. Phys. Solids 30, 1125 (1969).

[3] R. Emerald, R. Drews, and R. Zallen (unpublished).

[4] (a) P. Nielsen, Phys. Rev. B 10, 1673 (1974); (b) G. B. Fisher [in *Physics of Structurally Disordered Solids*, edited by S. S. Mitra (Plenum, London, 1975)] has reported the electronic structure of amorphous sulfur (not only S_8 rings) obtained by XPS.

[5] I. Chen, Phys. Rev. B 2, 1053 (1970); 2, 1060 (1970).

[6] D. J. Gibbons, Mol. Cryst. Liq. Cryst. 10 137 (1970).

[7] R. Boschi and W. Schmidt, Inorg. Nucl. Chem. Lett. 9, 643 (1973).

[8] N. V. Richardson and P. Weinberger, J. Electron. Spec. 6, 109 (1975).

[9] W. R. Salaneck, K. S. Liang, A. Paton, and N. O. Lipari, Bull. Am. Phys. Soc. 20, 402 (1975).

[10] J. A. Pople, D. P. Santry and G. A. Segal, J. Chem. Phys. 43, S129 (1965).

[11] L. Salem, *The Molecular Orbital Theory of Conjugated Systems*, (Benjamin, Reading, Mass., 1966), Chap. 2.

[12] J. C. Slater, Adv. Quantum Chem. 6, 1 (1972).

[13] K. H. Johnson, Adv. Quantum Chem. 7, 141 (1973).

[14] A. Streitweiser, Jr., *Molecular Orbital Theory for Organic Chemists* (Wiley, New York, 1961).

[15] H. F. Schaefer, *The Electronic Structure of Atoms and Molecules* (Addison-Wesley, Reading, Mass., 1972).

[16] M. J. S. Dewar, *The Molecular Orbital Theory of Organic Chemistry* (McGraw-Hill, New York, 1969).

[17] J. N. Murrell and A. J. Harget, *Semi-Empirical Self-Consistent-Field Molecular Orbital Theory of Molecules* (Wiley, London, 1972).

[18] R. M. Friedman, J. Electron. Spec. 5 501 (1974).

[19] C. C. Roothaan, Rev. Mod. Phys. 23, 69 (1951).

[20] N. O. Lipari, C. B. Duke, W. R. Salaneck, and L. B. Schein, J. Chem. Phys. (to be published).

[21] D. T. Clark, Tetrahedron 24, 2663 (1968).

[22] W. R. Salaneck, N. O. Lipari, W. McCain, and R. LaForce, Solid State Commun. 15, 1453 (1974); E.-K. Kortela, E. Suoninen, M. Karras and R. Manne have also studied $S(K_\beta)$ emission of S_8 using MO calculations [J. Physics B 5, 2032 (1972)].

[23] W. R. Salaneck, R. LaForce, W. McCain, and N. O. Lipari, Bull. Am. Phys. Soc. 19, 212 (1974).

[24] W. R. Salaneck, K. S. Liang, A. Paton, and N. O. Lipari, Phys. Rev. B (to be published).

[25] K. S. Liang, W. R. Salaneck, A. Paton, and N. O. Lipari, Bull. Am. Phys. Soc. 20, 402 (1975).

[26] J. M. Sichel and M. A. Whitehead, Theor. Chim. Acta 7, 32 (1967).

[27] U. Gelius, B. Roos, and P. Siegbahn, Chem. Phys. Lett. 4, 471 (1970).

[28] M. Wolfsberg and L. Helmholz, J. Chem. Phys. 20, 837 (1952).

[29] R. Pariser, J. Chem. Phys. 21, 568 (1953).

[30] S. C. Abrahams, Acta Crystallogr. 8, 661 (1955); A. Caron and J. Donohue, *ibid.* 14, 548 (1961).

[31] C. R. Brundle, M. B. Robin, and H. Basch, J. Chem. Phys. 53, 2196 (1970).

[32] D. A. Lowitz, J. Chem. Phys. 46, 4698 (1967).

[33] R. E. Honig, RCA Rev. 18, 195 (1957).

[34] J. Berkowitz, in Ref. 1, Chap. 7.

[35] Large clear-yellow sulfur crystals were obtained from Ward's Natural Science Establishment, Rochester, N.Y.

[36] G. Johansson, J. Gedman, A. Berndtsson, M. Klasson, and R. Nilsson, J. Electron. Spec. 2, 295 (1973).

[37] J. R. Platt, J. Chem. Phys. 17, 484 (1949).

[38] M. Schluter, J. D. Joannopoulos, and M. L. Cohen, Phys. Rev. Lett. 33, 89 (1974).

[39] E. Moser and W. B. Pearson, *Progress in Semiconductors* (Wiley, New York, 1960), Vol. 5, p. 104.

[40] M. Kastner, Phys. Rev. Lett. 28, 355 (1972).

[41] I. H. Hillier and V. R. Saunders, Chem. Phys. Lett. 4, 163 (1969).

[42] G. Burns, J. Chem. Phys. 41, 1521 (1964).

[43] R. Zallen, Phys. Rev. B 9, 4485 (1974).

[44] D. F. Hornig, J. Chem. Phys. 16, 1063 (1948); A. S. Davydov, Zh. Eksp. Teor. Fiz. 18, 201 (1948); H. W Winston and R. J. Halford, J. Chem. Phys. 17, 607 (1949).

[45] R. S. Halford, J. Chem. Phys. 14, 8 (1946).

[46] J. Donohue, in Ref. 1, Chap. 2.

[47] J. E. Baer and M. Carmack, J. Am. Chem. Soc. 71, 1215 (1949).